

# Simulation of Two-Phase Flows in a Stirred Mixing Tank

Zili Zhu and Nick Stokes

CSIRO Mathematical & Information Sciences,  
Private Bag 10, Clayton South MDC,  
Clayton, 3169, Australia

## ABSTRACT

A numerical model for simulating turbulent two-phase flows agitated by an impeller in a mixing tank is presented. An axi-symmetric model is used for the impeller blades and wall baffles. The two-phase fluid is modelled as a two-fluid interpenetrating gas-liquid mixtures. A RNG-based turbulence model is implemented in the numerical algorithm.

This numerical scheme is used to predict a turbulent two-phase gas-liquid flow in a stirred vessel for which experimental data has been gathered. The numerical method presented in this paper is validated against experimental data.

## 1. INTRODUCTION

Mixing is an essential engineering process in the mineral and metal processing industries. Gas-liquid two-phase flows are often used either as an integral part of mixing processes or to facilitate effective chemical reactions. Understanding the complex gas-liquid flows in agitated mixing tanks is vital to any efforts to improve such mixing processes. In this paper, we present a numerical method for simulating two-phase flows stirred by a impeller in a mixing vessel. The two-phase fluid is a mixture of liquid and gas, the impeller can be a Rushton turbine or a propeller. There are also baffles mounted inside the mixing tank. Such mixing tanks are widely used in the mineral and metal processing industries.

For agitated mixing tanks, the two-phase fluid flows are three-dimensional, and the flow is often turbulent under normal working condition. In addition, as the impeller blades rotate relative to the stationary baffles, we also face a rotating (moving) boundary situ-

ation. A direct numerical simulation of such complex unsteady three-dimensional turbulent two-phase flows would be prohibitively expensive in terms of computation time and computer memory. The cost in terms of human resources to prepare and to set up a model of a even very simple agitated mixing vessel will be much more than the computing expenses. Therefore, a simple and easy-to-implement mathematical model for simulating such two-phase flows is needed for engineers as their practical tool in assessing and for improving mixing processes.

In this paper, we first present a numerical scheme that can be easily implemented to simulate such two-phase flows in mixing tanks stirred by impellers. This numerical scheme will then be used to predict a liquid-air flow in a stirred mixing tank. The prediction given by the numerical method is compared with experimental results. The computation time and memory requirement for the simulation are within easy reach of ordinary workstations, and the robustness of the numerical method and accuracy of the predictions will be demonstrated. The numerical algorithm is implemented through general PDE package *Fastflo* (Zhu 1993).

## 2. MATHEMATICAL MODELS

### 2.1 Two-Phase Flow Model

For the two-phase flow in the mixing vessel, we consider the liquid to be the dominant component: i.e. liquid is regarded as the carrying medium. The volume fraction of the liquid is  $\alpha_l$ , and the gaseous fluid has a volume fraction of  $\alpha_g$ .  $\alpha_l$  and  $\alpha_g$  satisfy the relationship of  $\alpha_g + \alpha_l = 1$ .

We use a two-fluid model for the two-phase flows. The gas and liquid will have the same pressure field, but each phase has its

own velocity field. The interaction between the gas and liquid is reflected by an extra term in the momentum equations of the gas and liquid respectively. Therefore, a two-way coupling between the gas and liquid is fully implemented.

The governing equations of the turbulent two-phase flows consist of the Favre-averaged equations of conservation.

The mass continuity equation is:

$$\frac{\partial \alpha_k}{\partial t} + \nabla \cdot (\alpha_k \mathbf{V}_k) = 0 \quad (1)$$

where  $k$  indicates the  $k$ th phase of the fluid mixture.  $\mathbf{V}_k$  is the velocity vector of the  $k$ th phase of the fluid, the vector velocity  $\mathbf{V}_k$  has its component  $U_i^k$  in the  $i$  coordinate direction.  $\rho_k$  is the density of the  $k$ th phase.

The momentum equation is written as:

$$\rho_k \alpha_k \frac{\partial \mathbf{V}_k}{\partial t} + (\rho_k \alpha_k \mathbf{V}_k \cdot \nabla) \mathbf{V}_k + \frac{\alpha_k}{M^2} \nabla P - \nabla \cdot [\alpha_k \mu_t (\nabla \mathbf{V}_k + \nabla \mathbf{V}_k^T)] = \mathbf{L} - \mathbf{G} + \mathbf{F}_g \quad (2)$$

while  $P$  is the common pressure, and  $M^2 = \rho_0 U_0^2 / P_0$  is the Mach number, a coefficient resulting from non-dimensionalization. For incompressible fluid,  $M$  can be set to 1.  $\mu_t$  is the turbulent viscosity which will be defined later by a  $k - \epsilon$  turbulence model.

On the right hand side of the momentum equation,  $\mathbf{G}$  is the gravity vector force which acts on the fluid uniformly, while  $\mathbf{L}$  is a vector force that only has a constant value in the fluid region covered by the impeller blades. This vector force  $\mathbf{L}$  is created to represent the directional lifting force produced by propeller blades.  $\mathbf{F}_{gl}$  is the interacting force between the liquid and gas phases. In the current implementation,  $\mathbf{F}_{gl}$  consists of three components:

$$\mathbf{F}_{gl} = \mathbf{F}_{dk} + \mathbf{F}_{mk} + \mathbf{F}_{lk} \quad (3)$$

where  $\mathbf{F}_{dk}$  is the interfacial drag force on the  $k$ th phase,  $\mathbf{F}_{mk}$  is the added virtual mass force on the  $k$ th phase and  $\mathbf{F}_{lk}$  is the interfacial lift force on the  $k$ th phase.

The interfacial drag force  $\mathbf{F}_{dk}$  is calculated in the same way as that of Morud & Hjertager 1996:

$$\mathbf{F}_{dk} = F_d (\mathbf{V}_l - \mathbf{V}_k) \quad (4)$$

where the scalar coefficient  $F_d$  can be calculated from

$$F_d = \frac{3}{4} \alpha_l \alpha_g \rho_l \frac{C_d}{d_b} |\mathbf{V}_l - \mathbf{V}_k|$$

and

$$C_d = \frac{2}{3} d_b \sqrt{\frac{g \delta \rho}{\gamma}} \left[ \frac{1 + 17.67 [f(\alpha_g)]^{6/7}}{18.67 f(\alpha_g)} \right]^2$$

here

$$f(\alpha_g) = \begin{cases} (1 - \alpha_g)^{1.5} & \text{if } \alpha_g \leq 0.3 \\ \frac{8}{3} \alpha_l^2 & \text{if } 0.3 < \alpha_g \leq 0.7 \\ \alpha_g^3 & \text{if } \alpha_g > 0.7 \end{cases}$$

$$d_b = \frac{4}{\sqrt{g \delta \rho / \gamma}}$$

where  $g$  is the gravitational acceleration,  $\gamma = 0.07 \text{ kg/s}^2$  and  $\delta \rho = \rho_l - \rho_g$ .

The added virtual mass force  $\mathbf{F}_{mk}$  can be computed from the following formula (Boisson & Malin 1996):

$$\mathbf{F}_{mk} = \rho_l C_m \alpha_g \left[ \frac{\partial \mathbf{V}_g}{\partial t} + \mathbf{V}_g \cdot (\nabla \mathbf{V}_g) - \frac{\partial \mathbf{V}_l}{\partial t} - \mathbf{V}_l \cdot (\nabla \mathbf{V}_l) \right] \quad (5)$$

where the coefficient  $C_m$  is calculated from (Boisson & Malin 1996)

$$C_m = C_{ma} (1 - 2.78 \cdot \min\{0.2, \alpha_g\})$$

where  $C_{ma} = 0.5$ .

The interfacial lifting force  $\mathbf{F}_{lk}$  is calculated in the same way as that of Boisson & Malin (1996).

$$\mathbf{F}_{lk} = C_l \rho_l \alpha_g (\mathbf{V}_g - \mathbf{V}_l) \times (\nabla \times \mathbf{V}_l) \quad (6)$$

where  $C_l$  is assumed the same value as  $C_m$ .

Temperature  $T$  is assumed to be the same for both the liquid and the gas at any particular point in the space. The energy equation can therefore be written as:

$$\rho C_p \frac{\partial T}{\partial t} + \rho C_p \mathbf{V} \cdot \nabla T = \nabla \cdot [(C_p \mu_t + \lambda) \nabla T] + h_s \quad (7)$$

$h_s$  is the heat source due to the chemical reaction in the two-phase fluid. In this paper, we only assume that:

$$h_s = A \rho \alpha_l \alpha_g h_{\text{reac}} \left( \frac{T}{T_0} \right)^4$$

where  $h_{reac}$  is the heat of reaction,  $T_o$  is the ambient air temperature.  $C_p$  is the total specific heat of the fluid, and it can be calculated as:

$$C_p = \rho_l \alpha_l C_{pl} + \rho_g \alpha_g C_{pg}$$

where  $C_{pl}$  is the specific heat of the liquid, and  $C_{pg}$  is the specific heat of the gas.

## 2.2 $k - \epsilon$ Turbulence Model

We will use turbulence models developed for single-phase fluid flows to estimate turbulence effect in two-phase fluid flows. In the present paper, we will use the two-equation  $k - \epsilon$  model based on the Renormalization Group (RNG) analysis (Yakhot et al 1986). The velocity and density used in the turbulence model will be Favre-averaged.

$$\rho = \alpha_l \rho_l + \alpha_g \rho_g$$

$$\rho \mathbf{V} = \alpha_l \rho_l \mathbf{V}_l + \alpha_g \rho_g \mathbf{V}_g$$

The transport equation for the turbulence kinetic energy  $k$  is:

$$\rho \frac{\partial k}{\partial t} + \rho \mathbf{V} \cdot \nabla k - \nabla \cdot [\alpha \mu_t \nabla k] = \mu_t \sum_{i,j} \frac{\partial U_i}{\partial x_j} \left( \frac{\partial U_i}{\partial x_j} + \frac{\partial U_j}{\partial x_i} \right) - \rho \epsilon \quad (8)$$

and the dissipation rate  $\epsilon$  is:

$$\rho \frac{\partial \epsilon}{\partial t} + (\rho \mathbf{V}) \cdot \nabla \epsilon - \nabla \cdot [\alpha \mu_t \nabla \epsilon] = -\rho S + C_1 \nu_t \frac{\epsilon}{k} \sum_{i,j} \frac{\partial U_i}{\partial x_j} \left( \frac{\partial U_i}{\partial x_j} + \frac{\partial U_j}{\partial x_i} \right) - C_2 \rho \frac{\epsilon^2}{k} \quad (9)$$

Details of  $S$  can be found in the paper of Yakhot et. al. (1986). Once  $k$  and  $\epsilon$  are obtained, the total viscosity  $\mu_t$  is calculated from:

$$\mu_t = \rho \nu_{mol} \left[ 1 + \left( \frac{C_\mu}{\nu_{mol}} \right)^{1/2} \frac{k}{\epsilon^{1/2}} \right]^2 \quad (10)$$

The constants assume their standard values:  $C_\mu = 0.0845$ ,  $C_1 = 1.42$ ,  $C_2 = 1.68$ ,  $\beta = 0.012$ ,  $\eta_0 = 4.38$  and  $\alpha = 1.39$ .

## 2.3 Models of Impeller and Baffles

In this paper, we consider a generic mixing tank, where baffles are mounted on the tank's cylindrical wall, and an impeller rotates at constant angular speed in the center

of the tank. The tank is filled with liquid, and gas is released into the tank at a location along the axis, as shown in Figure 1.

In our mathematical model, the impeller is regarded as having infinite number of blades rotating at constant angular speed  $\omega$ . We also assume that there are also infinite number of baffle blades. With such a simplification, we can treat the flow as axisymmetric, and the flows and heat transfer can therefore be resolved in two dimensions. A cylindrical coordinate system  $(r, z, \theta)$  will be adopted, with the same axis as the mixing vessel.

When the axial velocity  $U_z$  and radial velocity  $U_r$  are determined from the momentum equation along the axial and radial directions, it should be noted that the momentum equation still applies within the region occupied by the impeller blades, but with the  $\theta$ -component equation replaced by one prescribing  $U_\theta$  as:  $U_\theta = \omega \times r$ . In the case of a propeller, an additional driving force that accounts for lifting effect will appear in the momentum equations. Of course, the surface of the impeller's blades has a damping effect on  $(U_r, U_z)$ , this can be modelled with a high viscous term being added to the momentum equation.

For the tangential velocity component, within the area occupied by the impeller blades, we regard  $U_\theta$  as that of a solid rotating body: i.e. the tangential velocity is determined as  $U_\theta = C_s [\omega \times r]$ , where  $C_s$  is a slip coefficient that is determined by the number of impeller blades. For the region outside the impeller blades, the tangential velocity  $U_\theta$  is determined from the momentum equation in the tangential direction  $\theta$ .

In the area that is occupied by the baffles, the tangential velocity  $U_\theta$  is assumed to be zero, while the momentum equations for  $(U_r, U_z)$  have an extra viscous term.

## 3. NUMERICAL SCHEME

To obtain the liquid velocity  $\mathbf{V}_l$ , we will use an artificial-compressibility method (Zhu 1993) to solve the liquid momentum equations. For the gaseous velocity  $\mathbf{V}_g$ , we will use a classical two-level convection-diffusion operator-splitting scheme (*Fastflo* Tutorial

Guide 1996). The operator-splitting scheme is based on separating the convection and diffusion terms of the momentum equations.

The velocities of both the gas and the liquid are solved separately and sequentially. The procedure for solving the two-phase fluid flow is iterative. The solution procedure for all the equations is listed in the following 12 steps:

1. The liquid momentum equation (2) in the tangential direction is solved to give  $U_\theta^l$ .
2. The momentum equations (2) for the liquid in the  $r$  and  $z$  directions are then solved to give  $(U_r^l, U_z^l)$ .
3. The pressure is then updated by solving the continuity equation for liquid.
4. The gas momentum equation (2) in the tangential direction is solved to give  $U_\theta^g$ .
5. The three interfacial forces between the gas and the liquid are evaluated by equations (4), (5), (6).
6. The two-step operator-splitting scheme is employed to solve the gas momentum equations (2) to give  $(U_r^g, U_z^g)$ .
7. In the operator-splitting scheme, the mass transport equation (1) for the gas is solved to give the distribution of gas volume fraction  $\alpha_g$ .
8. The pressure is updated again by solving the continuity equation for the gas.
9. The turbulence parameters  $k$  and  $\epsilon$  are obtained by solving their respective transport equations (8) and (9).
10. Total viscosity  $\mu_t$  is now updated by (10).
11. The three interfacial forces between the gas and the liquid are updated before another iterative loop is started.
12. The energy equation (7) is solved to obtain temperature distribution.

The entire numerical method is implemented in finite-element formulation using the general PDE package *Fastflo*.

## 6. NUMERICAL TEST

The numerical method presented in this paper will be verified for its robustness and accuracy. We have chosen the 151 stirred vessel of Applicon for which experimental data is available as published by Morud & Hjertager (1996). The schematic of the mixing tank with a six-bladed Rushton turbine and four

baffles is shown here in Figure 1.

The diameter of the vessel is  $D = 0.222$  m, and the impeller diameter is  $D_i = D/3$ . The baffle width is  $B = D/10$  and the Rushton turbine blades have a squared shape of  $L = 0.09D$  length. The blades are attached to a impeller disk of diameter  $0.243D$ . The disk is at height  $H = 0.47D$  from the bottom of the vessel. The gas is introduced to the tank through a pipe of diameter  $0.108D_i$ , the pipe inlet is located on the vessel axis and the distance between the pipe inlet and the bottom of the vessel is  $0.2D$ . The tank is filled with distilled water to the height of  $H_0 = D$ . The Rushton turbine is rotating at a speed of 360 RPM. The total volume of water in the vessel is 7.51 litres, and the rate of air flowing into the vessel is 1 vvm (volume air per volume liquid per minute).

As the two-phase flow is treated as axisymmetric, we only need to solve the two-phase flow in half of the cross-section of the mixing vessel. The mesh representing the discretized cross-section of the vessel is shown on the left side of Figure 2. The right half cross-section of Figure 2 shows the computed liquid velocity vector arrows. The air pipe is represented as a tube along the axis below the impeller. In the present simulation, we use 2000 grid points to cover half of the cross-section. Linear triangular elements are used. In the present calculation, after 24 hours of CPU time on a DEC 3000 alpha workstation, we can achieve convergence within 1700 iterations, and without any guessed solution to start from.

In Figure 3, we have plotted the computed radial and axial velocity components of the air at height  $H = 0.23D$ . Experimental results are also plotted in the figure for comparison (experimental data of the tangential (swirling) velocity component is not available). The radial velocity of the air is well predicted in the area of  $0.2 < r/R < 1.0$ , but in the region of  $r/R < 0.2$ , the radial velocity is under-predicted. The axial velocity component is over-predicted for a large part of  $r/R > 0.1$ , even though the general trend is well represented. For both radial and axial components, in the region  $r/R < 0.2$ , the computed results are largely influenced by the location of the bottom of the rotating

shaft of the impeller, since in the present setting, there is only very small gap between the bottom of the shaft and the air inlet. As we do not have precise data on the location of the bottom of the shaft, in the present computation, we choose  $H = 0.25D$  as the location of the bottom of the shaft, to approximately coincide with the published schematic. Once we have obtained exact data on the location, we expect the prediction could be improved in the range  $r/R < 0.2$ .

At height  $H = 0.47D$  from the bottom of the vessel (where the impeller disk is mounted), we compare the radial, axial and tangential components of the air velocity with the experimental data of Morud & Hjertager (1996). The results are presented here in Figure 4. As the impeller blades rotates at this height  $H = 0.47D$ , experimental data is not available within the rotating blade area of  $r/R < 0.333$ . In Figure 4, the numerical prediction for the radial velocity agrees well with experimental data, while the axial velocity is over-predicted. However, by examining the experimental measurement of the axial velocity of air, we can see that the axial velocity is almost zero everywhere radially. This indicates the air bubbles do not flow upwards in the experiment, a seemingly violation of air mass conservation. This discrepancy may be attributed to the fact that the circumferential averaged axial velocity in the experiment is not Favre averaged with volume fraction  $\alpha_g$ , while the numerical solution is based on Favre averaging. In other words, the experimental axial velocity has different meaning from the numerical axial velocity. It is not surprising to have such a discrepancy when they are compared. Experimental results based on Favre averaged data should be compared with the present numerical solution. The swirling velocity is moderately over-predicted, but the radial distribution of the swirling velocity is well simulated as shown in Figure 4.

As there is no temperature measurement in the experiment, we have not included computed temperature results.

## 7. CONCLUSION

In this paper, we have presented a nu-

merical method for predicting turbulent two-phase flows in an agitated mixing tank. The two-phase flows are made up of bulk liquid and air. The flows are driven by a Rushton turbine or a propeller.

The rotating impeller and stationary baffles are mathematically modelled to have infinite number of blades, so that the complex two-phase flows can be treated as axisymmetric. A convection diffusion operator-splitting technique is used to simulate the gaseous flow while the liquid velocity is determined by an artificial-compressibility method. A RNG-based  $k - \epsilon$  model is implemented to account for turbulence effect.

The numerical algorithm presented in this paper is used to predict an air-water two-phase flow driven by a six-blade Rushton turbine. The numerical solution of the radial, axial and tangential velocities of the air is compared with experimental results. However, a more valid comparison should be made when Favre-averaged experimental data can be found. From the comparison with the experimental data available, we can see that the present numerical method can well qualitatively predict the two-phase flow in regards to the gaseous velocity.

Given the complex nature of the two-phase flows instigated by an impeller, the accuracy of the predictions of the present numerical method is quite satisfactory. As experimental data is not available on the liquid velocity, we cannot evaluate the accuracy of predicting the velocity of the liquid flow.

As part of our continual research on flows driven by impellers, the next step will be to include solid particles to study three-phase flows in agitated mixing tanks. Solid particle suspension and heat transfer will be the focus of this research activity.

## ACKNOWLEDGMENTS

This research has been carried out as part of a Becher Aeration Research Project, in conjunction with the Divisions of Minerals and Building, Construction and Engineering, and supported by a CSIRO Priority-Project Funding Scheme. The two-phase flow algorithm is also developed as part of general PDE package *Fastflo*.

## REFERENCES

COMPUMOD 1996, Flexible Finite Element Software for Research Innovation and Design, Tutorial Guide, Computer Modelling in Engineering (COMPUMOD).

Boisson, N. and Malin M.R. 1996, Numerical Prediction of Two-Phase Flow in Bubble Columns, *Int. J. for Numerical Methods in Fluids*, Vol.23, pp.1289-1310.

Morud K.E. and Hjertager B.H. 1996, LDA

Measurements and CFD Modelling of Gas-Liquid Flow in a Stirred Vessel, *Chemical Engineering Sciences*, Vol.51, No.2, pp.233-249.

Yakhot, V. and S.A. Orszag, S.A., 1986, Renormalization Group Analysis of Turbulence: 1. Basic Theory, *J. Sci. Comput.*, Vol.1, No.3.

Zhu, Z. 1993, Artificial-Compressibility Method with Upwinding, *Computational Techniques and Applications: CTAC93*, World Scientific, pp.502-510.

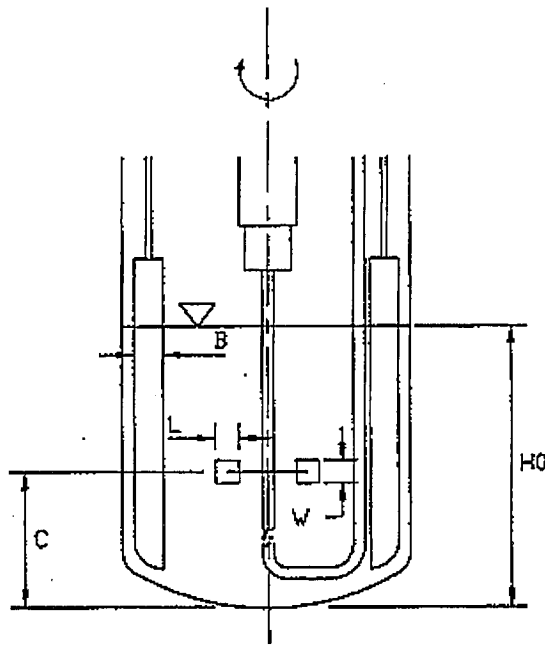


Figure 1: Schematic of the mixing tank with an impeller.

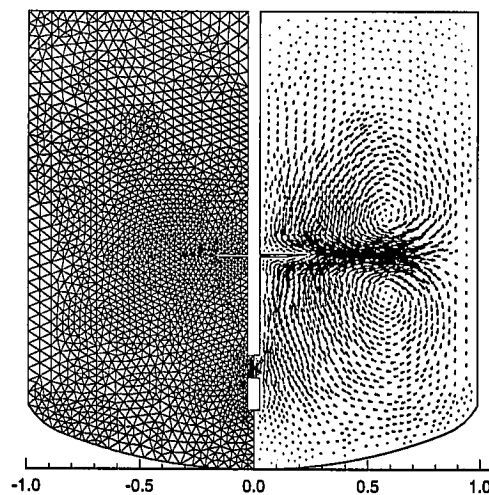


Figure 2: Mesh distribution and water velocity vector arrows in the cross-section.

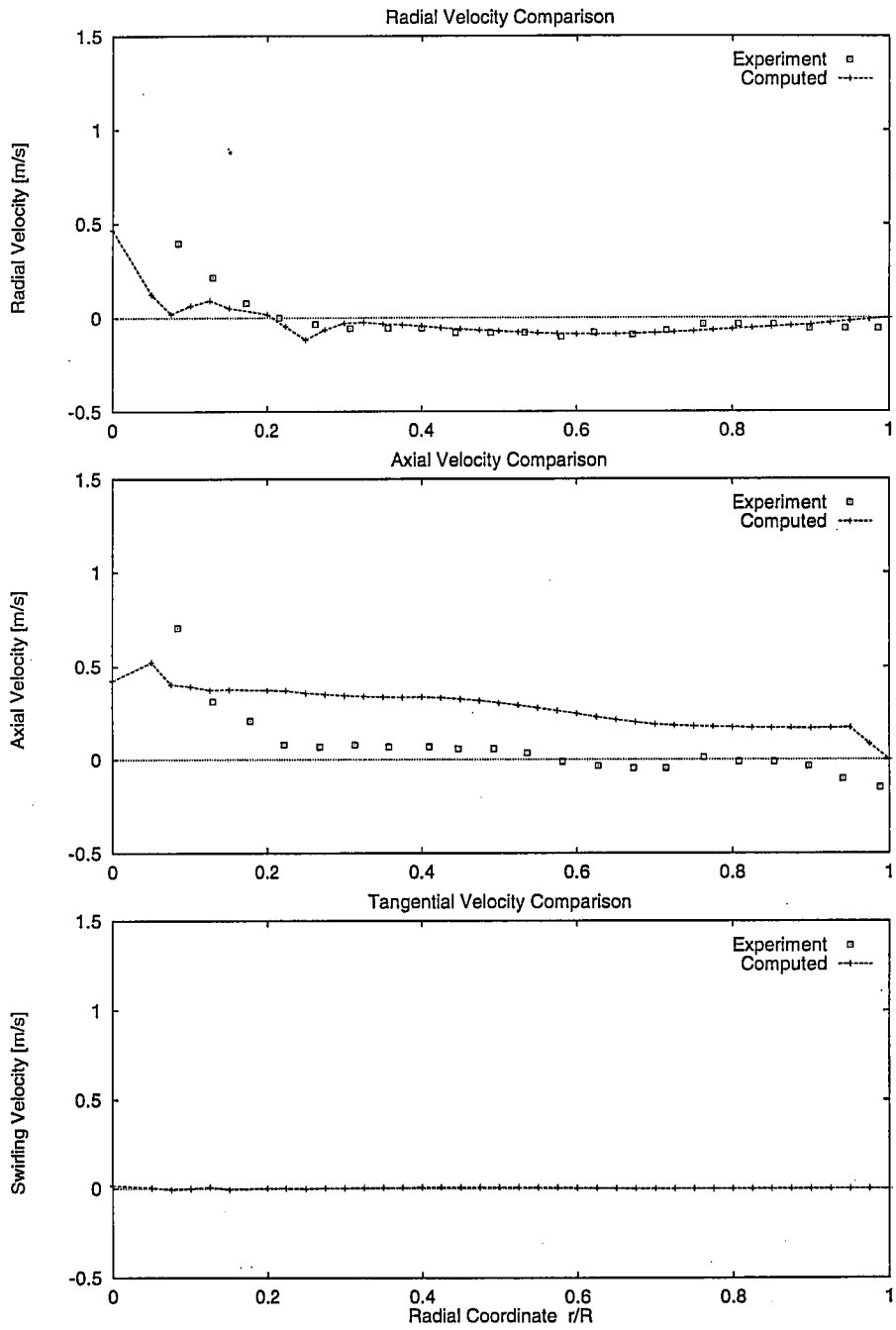


Figure 3: Comparison of air velocity profiles at axial location  $H = 0.23D$ .

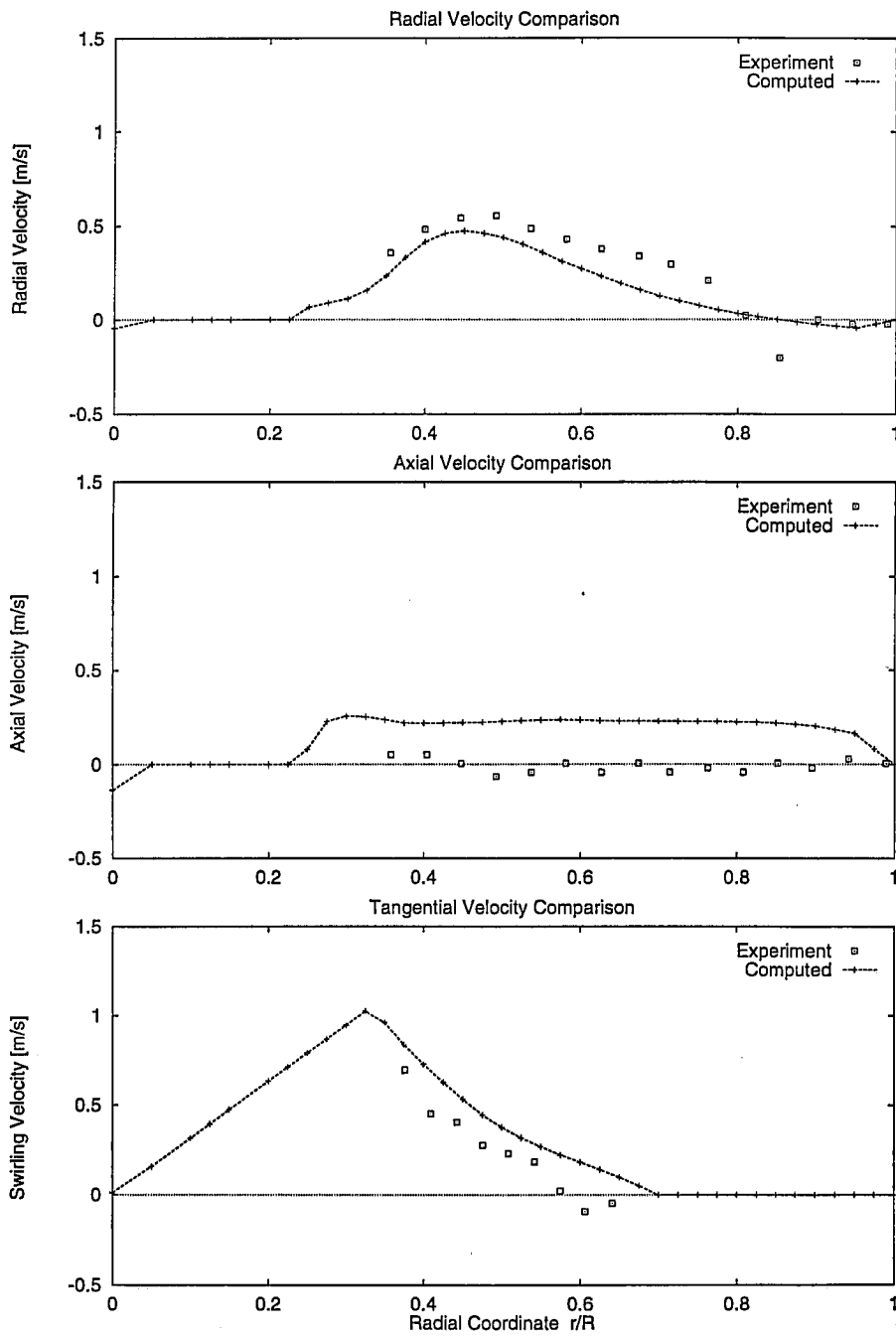


Figure 4: Comparison of air velocity profiles at axial location  $H = 0.47D$ .